

Variability of Young Massive Stars in the Galactic Super Star Cluster Westerlund 1

Alceste Z. Bonanos¹

ABSTRACT

This paper presents the first optical variability study of the Westerlund 1 super star cluster in search of massive eclipsing binary systems. A total of 129 new variable stars have been identified, including the discovery of 4 eclipsing binaries that are cluster members, 1 additional candidate, 8 field binaries, 19 field δ Scuti stars, 3 field W UMa eclipsing binaries, 13 other periodic variables and 81 long period or non-periodic variables. These include the known luminous blue variable, the B[e] star, 11 Wolf-Rayet stars, several supergiants, and other reddened stars that are likely members of Westerlund 1. The bright X-ray source corresponding to the Wolf-Rayet star WR77o (B) is found to be a 3.51 day eclipsing binary. The discovery of a reddened detached eclipsing binary system implies the first identification of main-sequence stars in Westerlund 1.

Subject headings: binaries: eclipsing, stars: Wolf-Rayet, stars: variables: other, open clusters and associations: individual (Westerlund 1)

1. Introduction

Westerlund 1 is a unique laboratory for studying the elusive evolution of massive stars. It has recently emerged as the nearest known super star cluster, i.e., a globular cluster precursor, typically found in starburst galaxies. Its discovery dates back to Westerlund (1961), however, the high amount of reddening ($A_V \sim 12$ mag) hindered spectroscopic observations for many years (see Westerlund 1987). Spectroscopy by Clark & Negueruela (2002) and Clark et al. (2005) revealed a massive stellar population of post-main sequence objects and determined it to be the most massive compact young cluster known in the Local Group. Mengel & Tacconi-Garman (2007) measured a dynamical mass of $\log M = 4.8$, in agreement with the mass inferred by Clark et al. (2005). Westerlund 1 therefore weighs more

¹Vera Rubin Fellow, Carnegie Institution of Washington, Department of Terrestrial Magnetism, 5241 Broad Branch Road NW, Washington, DC 20015; bonanos@dtm.ciw.edu

than the R136 or Arches clusters, however, with an inferred age of 4.5-5 Myr (Crowther et al. 2006), it is more similar in age to the Quintuplet and Center cluster. Furthermore, it is less obscured by dust than the Galactic Center clusters, which allows for observations in the optical and is ten times nearer than R136, which decreases crowding and blending effects by the same amount. Clark et al. (2005) obtained spectroscopy of 53 stars, which were all classified as post main-sequence objects, including blue supergiants, red supergiants, yellow hypergiants, a luminous blue variable and 14 Wolf-Rayet (WR) stars. Currently, 24 WR stars have been identified in Westerlund 1 (see Crowther et al. 2006, and references therein), concentrating 8% of the known galactic WR stars in one cluster (van der Hucht 2006). *Chandra* observations have revealed the presence of a magnetar in Westerlund 1 (Muno et al. 2006), which for the first time places a firm lower limit on the mass of a neutron star progenitor. In addition, 12 WR stars and a B[e] star were found to be X-ray sources (Skinner et al. 2006).

The motivation behind this paper is twofold: to discover eclipsing binaries containing massive stars ($> 50 M_{\odot}$) and to provide time domain information for this remarkable cluster. Eclipsing binaries are extremely powerful tools that can be used to measure the most massive stars, probe the upper stellar mass limit and provide accurate masses and radii for the most massive stars in a variety of environments and at a range of metallicities. Double-lined spectroscopic binary systems exhibiting eclipses in their light curves provide accurate geometric measurements of the fundamental parameters of their component stars. Specifically, the light curve provides the orbital period, inclination, eccentricity, the fractional radii and flux ratio of the two stars. The radial velocity semi-amplitudes determine the mass ratio; the individual masses can be solved using Kepler's third law. Furthermore, by fitting synthetic spectra to the observed ones, one can infer the effective temperatures of the stars, solve for their luminosities and derive the distance (e.g. Bonanos et al. 2006).

Until recently, the most massive stars measured in eclipsing binaries were R136-38 in the Large Magellanic Cloud ($56.9 \pm 0.6 M_{\odot}$, Massey et al. 2002) and WR 22 ($55.3 \pm 7.3 M_{\odot}$, Rauw et al. 1996; Schweickhardt et al. 1999), an evolved star in our Galaxy. The current heavyweight champion is a galactic WR binary, WR 20a (Rauw et al. 2004; Bonanos et al. 2004), in the young compact cluster Westerlund 2, with component masses $83.0 \pm 5.0 M_{\odot}$ and $82.0 \pm 5.0 M_{\odot}$, making this the most massive binary known with an accurate mass determination. Such systems are of particular interest, since massive binaries might be progenitors of gamma-ray bursts (GRBs, e.g. Fryer et al. 2007), especially in the case of Population III, metal-free stars (see Bromm & Loeb 2006). They also provide constraints for untested massive star formation and evolution models, stellar atmosphere and wind models. Accurate parameters of massive stars provide insights into the frequency of “twin” binaries (see Pinsonneault & Stanek 2006; Krumholz & Thompson 2006), the progenitors of

X-ray binaries, core-collapse supernovae, the connection between supernovae and GRBs, and Population III stars, by studying any observed trends with metallicity.

A systematic search for the most massive stars ($> 50M_{\odot}$) in eclipsing binaries is currently underway. Analogs of WR 20a, if not more massive binaries, are bound to exist in the young massive clusters at the center of the Galaxy (Center, Arches, Quintuplet; e.g. Peeples et al. 2007), in nearby super star clusters (e.g. Westerlund 1 and R136), in Local Group galaxies (e.g. LMC, SMC, M31, M33) and beyond (e.g. M81, M83, NGC 2403). The large binary fraction (> 0.6) measured by Kobulnicky et al. (2006) among early-type stars in the Cygnus OB2 association implies that a significant number of massive short-period eclipsing binaries should exist in massive clusters. The first step in measuring accurate masses of the most massive stars involves discovering eclipsing binaries in massive clusters and nearby galaxies. The brightest of these are expected to contain very massive stars, and follow-up spectroscopy provides fundamental parameters for the component stars.

This paper presents the first variability study of the massive Westerlund 1 cluster, in search of massive stars in eclipsing binaries. It is organized as follows: §2 describes the observations, §3 the data reduction, calibration and astrometry, §4 the variable star catalog, §5 the color magnitude diagram and §6 the summary.

2. Observations

Photometry of Westerlund 1 was obtained with the Direct CCD on the 1 m Swope telescope at Las Campanas Observatory, Chile. The camera uses a 2048×3150 SITe CCD with a pixel size of $15\mu\text{m}$ pixel $^{-1}$ and a pixel scale of $0''.435$ pixel $^{-1}$. A 1200×1200 section of the CCD corresponding to $8.7'$ on the side was read out, centered at $\alpha = 16:47:03.8, \delta = -45:50:41$, J2000.0. The observations were made on 17 nights between UT 2006 June 15 and July 25, typically in *IRVB* sequences. The total number of exposures were $252 \times 5\text{s}$ and $216 \times 30\text{s}$ in the *I* filter, $217 \times 30\text{s}$ in *R*, $200 \times 600\text{s}$ in *V*, and $167 \times 1200\text{s}$ in *B*. Two exposure times were taken in *I* to increase the sensitivity to both bright and faint cluster members. The median value of the seeing was $1.2''$ in *I*, $1.3''$ in *R*, and $1.4''$ in both *V* and *B*. Westerlund 1 was observed at airmasses ranging from 1.04 to 2.69 in *I*, with the median being 1.16.

3. Data Reduction, Calibration and Astrometry

The images were processed with standard IRAF¹ routines. Specifically, the images were overscan corrected and trimmed, corrected for the non-linearity of the CCD with *irred.irlincor* in IRAF following Hamuy et al. (2006), and then flat fielded. The value of 23,000 ADU, above which the non-linearity has not been measured, was adopted to be the saturation limit in the following reductions.

3.1. Image Subtraction

The photometry of the variable stars was extracted using the ISIS image subtraction package (Alard & Lupton 1998; Alard 2000), which works well in crowded fields (see Bonanos & Stanek 2003). In each filter, all the frames were transformed to a common coordinate grid and a reference image was created by stacking several frames with the best seeing. For each frame, the reference image was convolved with a kernel to match its PSF and then subtracted. On the subtracted images, the constant stars cancel out, and only the signal from variable stars remains. A median image of all the subtracted images was constructed, and the variable stars were identified as bright peaks on it by visual inspection. Finally, profile photometry was extracted from the subtracted images.

DAOPHOT/ALLSTAR PSF photometry (Stetson 1987) was performed on the single template images separately and the flux scaling was corrected when transforming to magnitudes, as described in Hartman et al. (2004). A more detailed description of the calibration is presented in §3.2.

3.2. Photometric Calibration

On two photometric nights, Landolt (1992) standard fields were observed to calibrate the *BVRI* light curves to standard Johnson-Kron-Cousins photometric bands. Specifically, the SA107, SA 109, PG1323, PG1525 fields were observed on UT 2006 June 19 (N04), covering a range in airmass from 1.07 to 1.86, and the MarkA, PG0231, PG1633 fields on UT 2006 July 19 (N12), covering a range in airmass from 1.07 to 2.10.

The transformation from the instrumental to the standard system was derived using the IRAF *photcal* package according to the equations:

¹IRAF is distributed by the National Optical Astronomy Observatory, which are operated by the Association of Universities for Research in Astronomy, Inc., under cooperative agreement with the NSF.

$$\begin{aligned}
 b &= B + \chi_b + \kappa_b \cdot X + \xi_b \cdot (B - V) \\
 v_1 &= V + \chi_{v11} + \kappa_{v12} \cdot X + \xi_{v13} \cdot (B - V) \\
 v_2 &= V + \chi_{v21} + \kappa_{v22} \cdot X + \xi_{v23} \cdot (V - I) \\
 r &= R + \chi_r + \kappa_r \cdot X + \xi_r \cdot (V - R) \\
 i &= I + \chi_i + \kappa_i \cdot X + \xi_i \cdot (V - I)
 \end{aligned}$$

where lowercase letters correspond to the instrumental magnitudes, uppercase letters to standard magnitudes, X is the airmass, χ is the zeropoint, ξ the color and κ the airmass coefficient. Additional bright red stars in the observed fields from the catalog of Stetson (2000) increased the color range for N04 to $-0.22 < B - V < 1.90$ mag using 95 stars and in N12 to $-0.33 < B - V < 1.53$ mag using 58 stars. Table 1 presents both photometric solutions. The solution of N04 has a larger number of stars, a greater color range and is in agreement with the values of the B, V color and extinction coefficients measured by Hamuy et al. (2006); it was therefore adopted. The transformation was repeated iteratively to determine the colors of the stars. The lack of observed standard stars with $B - V > 2$ mag limits the accuracy of the photometry for the reddest stars. A comparison with the photometry of P. Stetson (priv. comm.) presented by Clark et al. (2005) shows mean differences (Bonanos–Stetson) for the 100 brightest stars in common of -0.03 ± 0.04 mag in B , -0.01 ± 0.06 mag in V , 0.08 ± 0.08 mag in R and 0.24 ± 0.10 mag in I . The large offsets in R and especially in I are due to the lack of very red standards. The photometry was therefore scaled by these offsets in these two bands.

The completeness of the photometry starts to drop rapidly at about 18.5 mag in I , 20 mag in R , 21.5 mag in V and 22.5 mag in B . The CCD saturates for stars brighter than 10.75 mag in I for the short exposures and 12.3 mag in the long ones, 12.7 mag in R , 15.0 mag in V and 16.4 mag in B . The light curves of variables brighter than 12.3 mag in I were measured from the short exposure images.

The conversion of the variable star light curves to magnitudes involves two steps. First, it requires a conversion to instrumental magnitudes that takes into account the aperture correction measured on the template frame, to achieve correct scaling of fluxes and, consequently, correct amplitudes for the variables. This requires matching the variables with stars having DAOPHOT PSF photometry. In the few cases without matches, the light curves are presented in flux units. The conversion to the standard system involves an iterative color determination, which in turn requires detection of the variables in multiple filters. This was not the case for a large fraction of the stars; therefore, the following cluster colors $B - V = 3.8$ mag, $V - I = 5.0$ mag, $V - R = 2.8$ mag were adopted for the conversion, which are average

colors for the Westerlund 1 stars of interest. Hence, the photometry of the variable field stars is systematically offset by as much as 0.2 mag. Using these colors, the zeropoints were computed and added to the lightcurves. The I and R light curves were subsequently scaled to Stetson’s photometry.

3.3. Astrometry

Equatorial coordinates were determined for the I star list. The transformation from rectangular to equatorial coordinates was derived using 940 transformation stars with $V < 20$ from the USNO-B1.0 (Monet et al. 2003) catalog. The median difference between the catalog and the computed coordinates for over 700 transformation stars was $0.^{\prime\prime}2$.

4. Variable Star Catalog

The $BVRI$ light curves were searched separately for variability using the multiharmonic analysis of variance method (Schwarzenberg-Czerny 1996) and then merged. A total of 129 variables were found in the $8.7' \times 8.7'$ region centered on Westerlund 1, many of these being members of the Westerlund 1 cluster. The variables were classified by visual inspection into the following five categories: (detached) eclipsing binaries or (D)EBs for binaries with periods $P > 1$ day, W Ursae Majoris (W UMa) contact binaries for $P < 1$ day and amplitudes > 0.2 mag, δ Scuti for short period ($P < 0.2$ day) variables with amplitudes ~ 0.1 mag, periodic variables ($P > 0.2$ day), and “Other” that includes the long period or non-periodic variables. Table 2 presents the variable star catalog. It lists the name of the star given by Westerlund (1987), if available, or the revised identification given by Clark et al. (2005), the RA and Dec coordinates for J2000.0, the B , V , R , I intensity-averaged magnitudes, the spectral classification when available from Clark et al. (2005) and for the WR variables from Crowther et al. (2006), the light curve classification, and period when applicable. Variables with X-ray detections by Skinner et al. (2006) have an “X” following their WR classification. Note, that the catalog includes photometry for some stars that are missing from Clark et al. (2005) due to the gap between their two CCDs and their smaller field of view. Table 3 presents the light curves of the variables. The name of each star is based on its J2000.0 equatorial coordinates, in the format: $hhmmss.s+ddmmss.s$. In five cases, the light curve is available only in differential flux units.

The classification results yield 13 eclipsing binaries, 4 of which, and possibly 5, belong to Westerlund 1, 3 field W UMa binaries, 19 field δ Scuti variables, 13 other variables exhibiting periodic variability, and 81 variables that are either long period variables or non-periodic variables. Because of the degeneracy in distinguishing between W UMa and δ Scuti stars from photometry alone, a question mark is given with these classifications. SX Phe stars are

also short period pulsating stars in the classical instability strip, but belong to Population II and are unlikely to be found in the galactic disk.

Figure 1 presents the I –band reference image (0. $''$ 9 seeing) with the positions of the cluster eclipsing binaries and variable Wolf-Rayet stars. The eclipsing binaries belonging to Westerlund 1 were selected from the phased light curves as reddened eclipsing binaries with periods greater than a day. The location of the reddened DEB and WR77aa (T) demonstrate the extent of the cluster.

4.1. Eclipsing Binaries in Westerlund 1

Figure 2 presents phased light curves of the 5 newly discovered eclipsing binaries in Westerlund 1, in order of decreasing brightness in I . The 9.2 day binary (W13, or star 13 in the catalog of Westerlund 1987) is more than a magnitude brighter than the other eclipsing systems in I (see Table 2) and thus an excellent massive star candidate. Clark et al. (2005) assigned a spectroscopic identification of “OB binary/blend” for W13, which is in agreement with the contact eclipsing binary light curve shape. The second brightest system (W36), with the 3.18 day period, has a light curve resembling a near-contact configuration that is very accurate, thus lends itself to accurate parameter determination. There is no published spectroscopy for W36, but its red color and location, together with W13, in the core of the cluster give strong evidence for cluster membership.

The third system, WR77o (B), is a suspected binary from X-ray observations. Skinner et al. (2006) detected strong, hard X-ray emission with *Chandra* observations as well as low-amplitude variability in its X-ray light curve and concluded it is a likely binary. These data confirm their suspicion, as well as show it to be an eclipsing binary with a 3.51 day period. The eclipses give it additional value, as they allow future measurement of the radii and masses of the component stars of this WN7 system. The uneven out-of-eclipse light curve implies non-uniform surface brightesses of the component stars, whereas the uneven eclipse depths imply different temperatures. The brightening right before and after the secondary eclipse is suggestive of a bright spot, possibly arising near the L1 Lagrangian point and due to shocked colliding winds.

The fourth system, a 4.43 day detached eclipsing binary in an eccentric orbit, is the first main sequence object to be identified in Westerlund 1, as the detached configuration requires unevolved stars. It is located far from the cluster core, $\sim 4'$ south of the cluster, yet its colors are as reddened ($V - I = 5.5$ mag) as the cluster stars, indicating membership in the cluster. Similarly, WR77aa (T), at an even greater projected distance from the cluster center, is a member of Westerlund 1 (see Figure 1). Measuring the masses of the above binary component stars will additionally determine the extent of mass segregation for the

most massive stars in this super star cluster. Finally, the fifth eclipsing binary system found in Westerlund 1 has an extremely reddened color of $R - I = 3.7$ mag, is very faint ($R = 19.9$ mag), and shows small-amplitude variability with a period of 2.26 days. Cluster membership of this star needs to be confirmed. It is located near the cluster core, however the R -band light curve is too noisy to check whether the variation in amplitude is the same as in I -band, which is the case for eclipsing systems. It could alternatively be an extremely reddened pulsating or eclipsing field star.

It would be premature to draw any conclusions about the binarity fraction from this data alone, since the monitoring baseline was only sensitive to short period eclipsing binaries. Spectroscopic monitoring will reveal additional non-eclipsing systems and, along with X-ray and radio observations, will yield a more complete estimate of the binary fraction in Westerlund 1, already estimated by Crowther et al. (2006) to be $> 60\%$ for the Wolf-Rayet stars.

4.2. Wolf-Rayet Variables in Westerlund 1

Half of the 24 known Wolf-Rayet variables show significant optical variability, ranging from 0.05-0.4 mag. Most notably, WR77o (B), a WN7o type, is a 3.51 day period eclipsing binary with an eclipse depth of 0.2 mag, discussed in § 4.1. The other 11 Wolf-Rayet variable stars are: WR77sc (A), WR77sb (O), WR77r (D), WR77q (R), WR77p (E), WR77n (F), WR77k (L), WR77j (G), WR77i (M), WR77f (S), WR77aa (T). Figures 3 and 4 present light curves of the 12 variable WR stars. Skinner et al. (2006) have detected X-ray emission in 9 of these 12 variable Wolf-Rayet stars, which correspond to the WR stars with the largest variability amplitudes and are marked with an “X” in Figures 3 and 4. WR77f (S), with a WN10 – 11h/B0 – 1Ia+ spectral type, is an exception. It varies by ~ 0.2 mag, yet is not an X-ray source. WR77sc (A) shows a sharp 0.15 mag increase in brightness that roughly phases with a period of 7.63 days. Skinner et al. (2006) conclude that both WR77o (B) and WR77sc (A) are binaries from their high X-ray luminosity. Eclipses are not visible in the light curve of WR77sc (A), however the periodic variability is likely related to winds.

The low-amplitude variability (0.05-0.1 mag) observed in the rest of the WR stars qualitatively resembles the light curve behavior of WR 123 (WN8), monitored by the MOST satellite (Lefèvre et al. 2005) and is likely due to inhomogeneities in the winds. The present data are not sufficient for determining whether a periodic signal is present, similar to the 9.8 hour signal found in WR 123. The cause of this periodicity is not well understood. Dorfi et al. (2006) proposed that pulsations in hydrogen rich envelopes of stars with high luminosity to mass ratios are a possible explanation. Future monitoring of Westerlund 1, yielding simultaneously light curves of (at least) 24 Wolf-Rayet stars, will help in resolving the nature of the variability.

4.3. Other Variables

The other periodic variables include 7 field detached eclipsing binary systems, 2 of which are eccentric, and 1 semi-detached or contact binary shown in Figure 5. The non-detached field system, with a 6.862 day period, exhibits an uneven light curve that suggests it is a magnetically active RS CVn binary. There are also 9 field small-amplitude variables with $P > 0.2$ days (see Figure 6), 19 field small-amplitude variables with $P < 0.2$ (see Figure 7), and 4 semi-regular variables. These include WR77sc (A) ($P = 7.63$ days) and W6, an OB supergiant displaying a 2.2 day periodicity with a 0.2 mag amplitude. Many of the δ Scuti variables show significant scatter in their light curves, indicative of multiple mode pulsations that are typical in such stars.

A large fraction of the remaining 81 variables classified as “Other” have red colors, and can therefore help in identifying additional supergiants and other massive stars that are cluster members. Figure 8 shows light curves of 6 selected cluster members: the LBV, the B[e] star, and four blue supergiants.

5. Color Magnitude Diagram

Figure 9 presents the R vs. $R - I$ color-magnitude diagram (CMD), indicating the positions of the variables and in particular the eclipsing binaries in the cluster. Field stars are mainly located on the blue main sequence, whereas the Westerlund 1 stars have reddened colors between $2.2 < R - I < 3.2$ mag. The sparse second main-sequence identified by Clark et al. (2005) is also observed. It contains several variables, including the possibly magnetically active RS CVn eclipsing binary ($P = 6.862$ days), which is consistent with this group of stars being reddened by an intervening absorber. The brightest cluster eclipsing binary (W13) is remarkably bright, similar in brightness to the OB supergiants. Although a magnitude fainter, the second brightest EB (W36) is also located near OB supergiants on the CMD. The cluster DEB has a similar magnitude to WR77o (B); its position on the CMD is consistent with it being a cluster member. Spectral classification is required to confirm membership of the faintest EB. From their position on the CMD, the 4 semi-regular variables are likely cluster members; 2 of these (W6 and W72) have early-type spectral classifications and the brightest corresponds to W53.

There is definite contamination from the classical instability strip, as several δ Scuti variables occupy the same location as the cluster members. The 1.3 day variable with a 0.1 mag I -band amplitude at $R - I = 2.7, R = 15.9$ mag could be a subgiant FK Comae star. These rapidly rotating G-K stars are thought to form from coalesced W UMa binaries (see Bopp & Stencel 1981). Finally, the bright periodic variables with periods of 3.7 days ($R - I = 1.55, R = 16.3$ mag) and 3.715 days ($R - I = 0.9, R = 14.6$ mag) could alternatively be low-inclination contact binaries with 7.4 day periods.

6. Summary

This paper presents the first variability study of the Westerlund 1 cluster and is the first of a series of papers in search of the most massive stars ($> 50M_{\odot}$) in eclipsing binaries in young massive galactic clusters. A total of 129 variable stars are presented, including cluster supergiant and Wolf-Rayet star light curves, 4 (plus 1 candidate) cluster eclipsing binaries suitable for follow-up spectroscopy, 8 field eclipsing binaries, 19 pulsating δ Scuti variables, 3 W UMa eclipsing binaries, 13 other periodic variables and 81 long period or non-periodic variables. A significant number of the long period or non-periodic variables have red colors, suggesting cluster membership.

The discovery of 4 or 5 eclipsing binaries belonging to Westerlund 1 is significant, as it provides the means of measuring accurate masses and radii for these stars. The brightest of these has $V = 17.554$, $R = 14.707$, $I = 12.044$ mag, therefore its radial velocity curve is measurable with 4-6 meter class telescopes. Future determination of the Wolf-Rayet eclipsing binary parameters will be especially useful for understanding WN7 spectral type stars and probing their evolutionary state. The cluster detached eclipsing binary is the first main sequence object to be identified in Westerlund 1 and its location outside the cluster core may provide insights into cluster formation and evolution.

A systematic search for the most massive stars in eclipsing binaries in young massive clusters is efficient in discovering massive candidates, as shown to be the case in Westerlund 1. Radial velocity surveys are necessary for discovering non-eclipsing systems, however, they require large amounts of time on 6-8 meter class telescopes to identify binary candidates and obtain radial velocity curves. Photometric monitoring can be done using 1-2 meter telescopes and can easily identify short-period massive eclipsing binary candidates for follow-up spectroscopy. Eclipsing binary systems are thus extremely valuable probes of the most massive stars and can yield fundamental parameters of the most massive stars in both young massive clusters and nearby galaxies.

I am very grateful to Craig Heinke for bringing Westerlund 1 to my attention and thus motivating this variability study. Many thanks to Peter Stetson for providing his unpublished photometry of Westerlund 1, to Lucas Macri for help with the photometric calibration, to Kris Stanek for useful discussions and comments on the manuscript, and Stella Kafka for a careful reading of the manuscript. I acknowledge research and travel support from the Carnegie Institution of Washington through a Vera Rubin Fellowship.

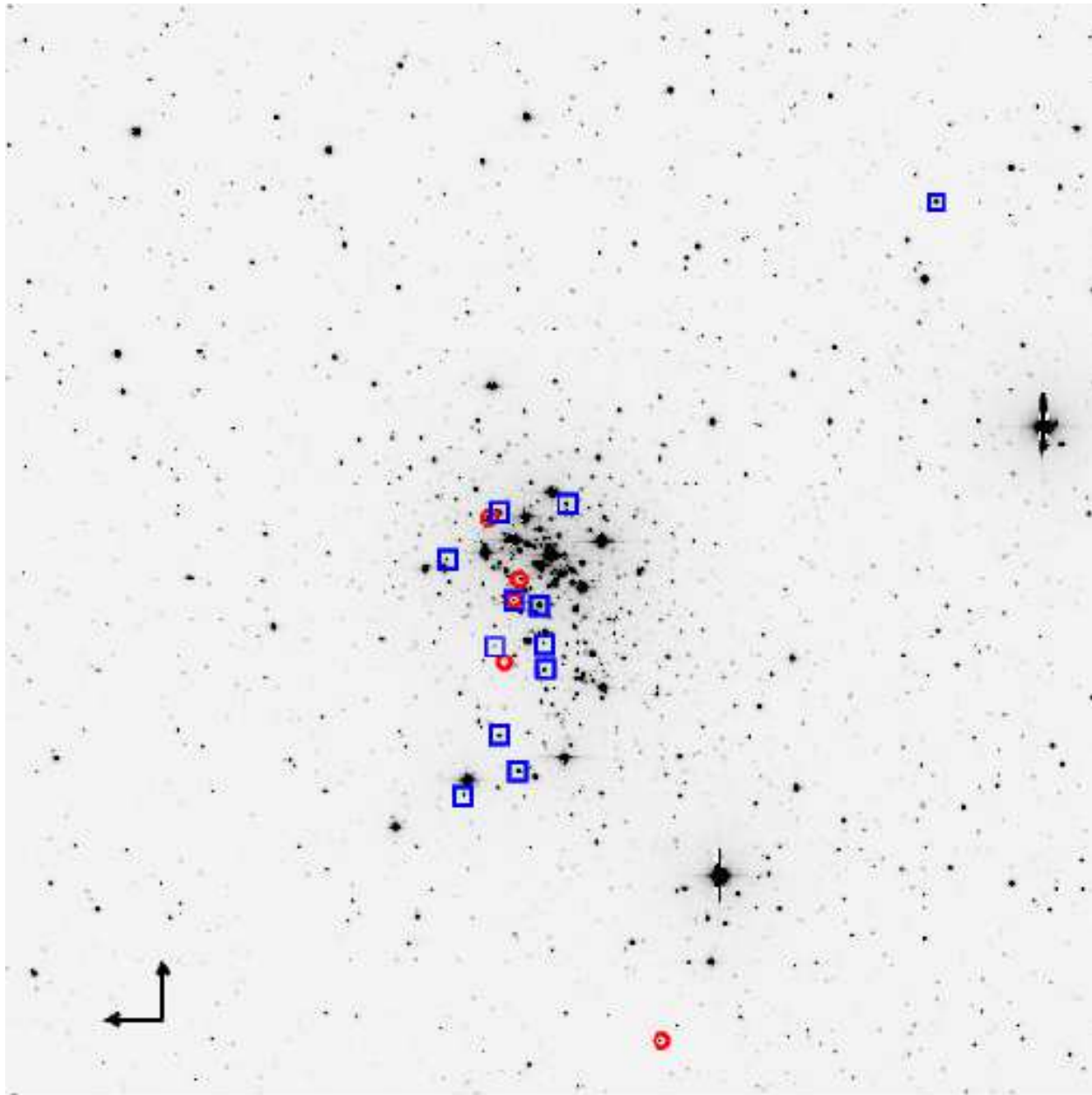


Fig. 1.— I –band finderchart of the observed $8.7' \times 8.7'$ field of Westerlund 1 ($0.^{\circ}9$ seeing). North is up and East to the left. Cluster eclipsing binaries are marked with red circles and variable Wolf-Rayet stars are marked with blue squares. Note, the large projected distances of the cluster DEB and WR77aa (T).

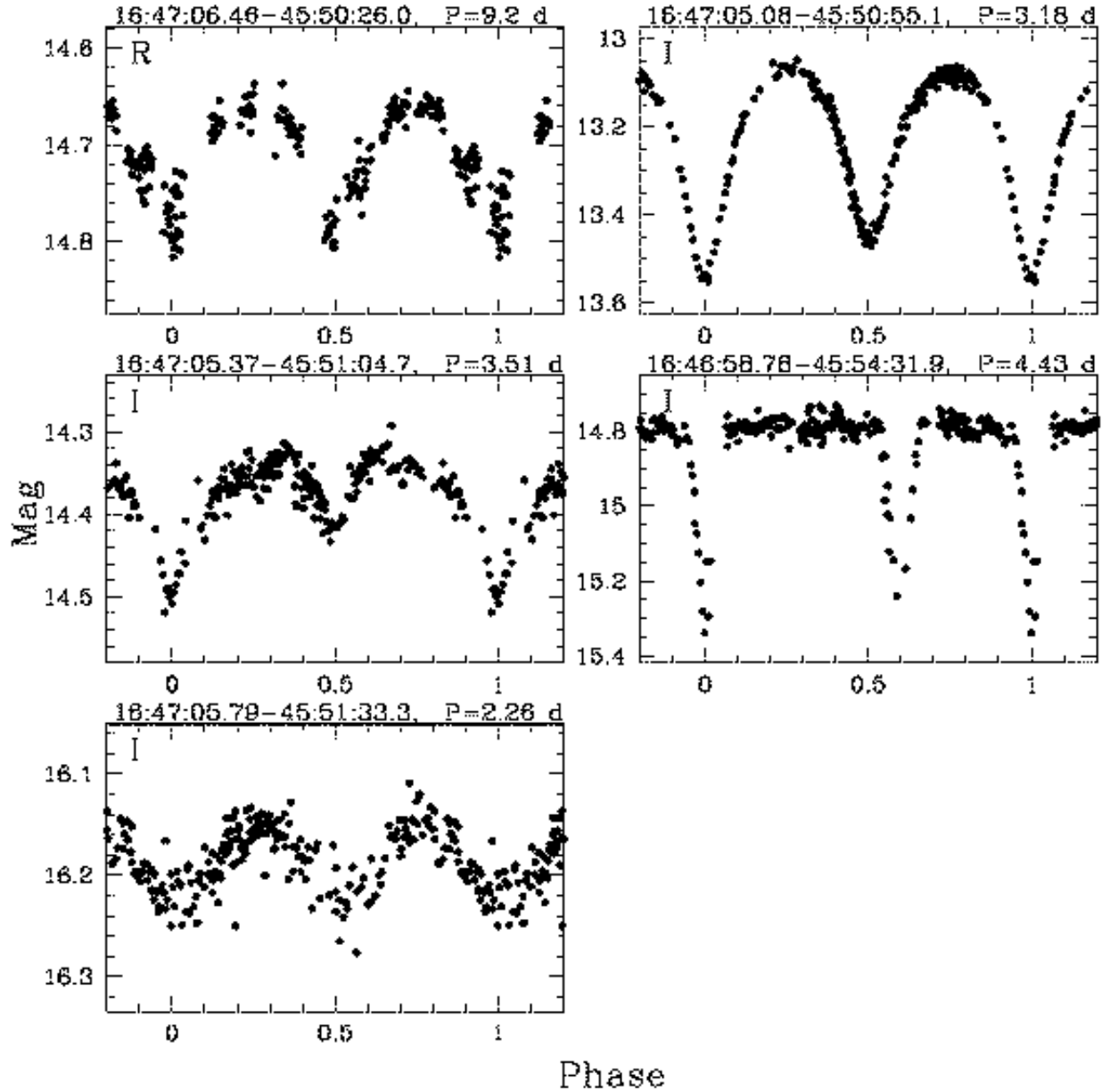


Fig. 2.— Phased light curves of the 5 eclipsing binary members of Westerlund 1, in order of decreasing brightness in I -band. The (RA, Dec) coordinates, periods and filters are labelled. The 3.51 day system corresponds to WR77o (B). Cluster membership of the faintest system needs to be confirmed.

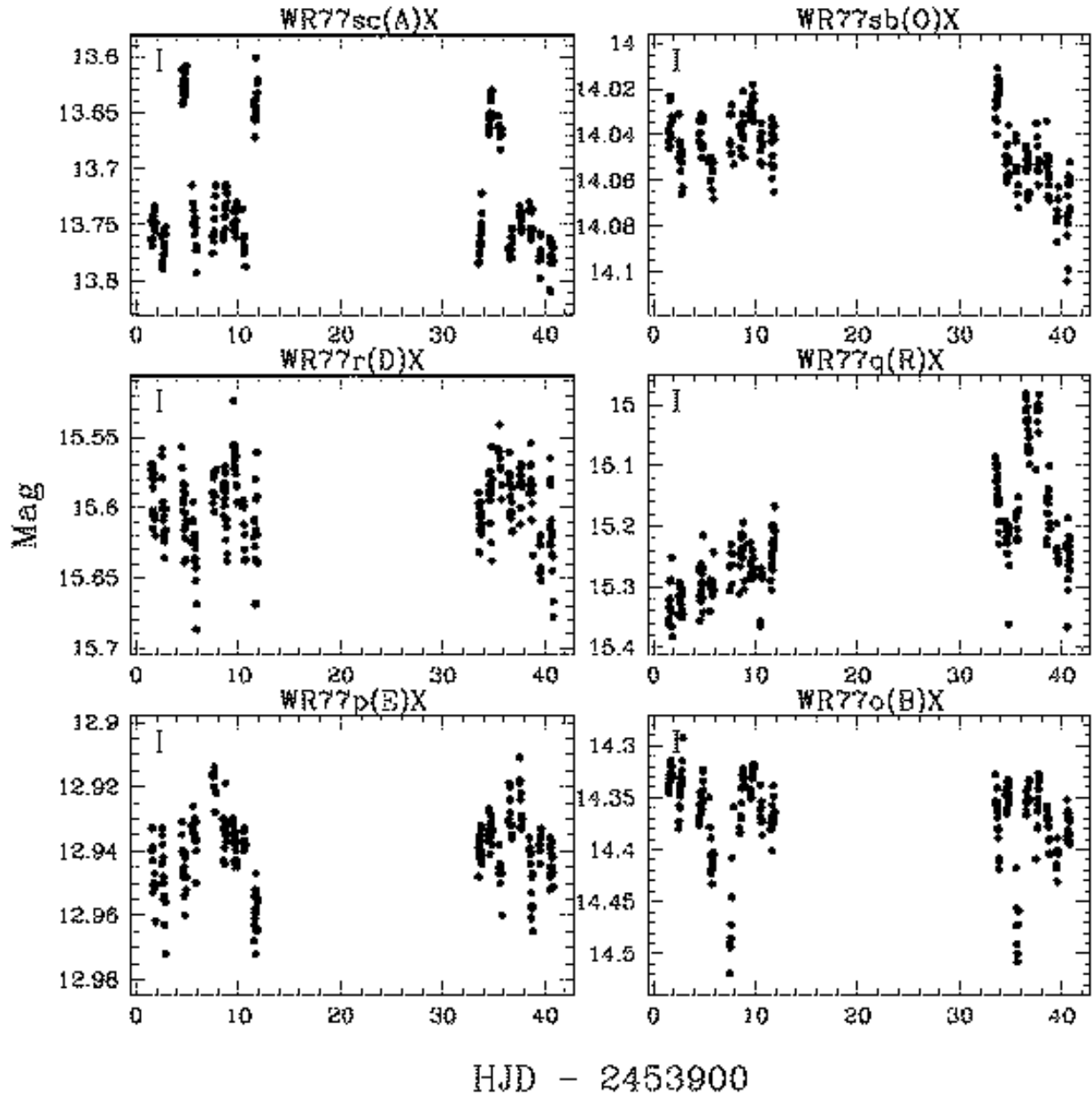


Fig. 3.— Light curves of 6 variable Wolf-Rayet members of Westerlund 1. The new name designations (van der Hucht 2006) are followed in parentheses by the letter names (Clark et al. 2005). An “X” is appended for sources with X-ray detections from *Chandra* (Skinner et al. 2006). The plotted filter is labelled in each panel. The phased light curve of the eclipsing binary WR77o (B) is shown in Figure 2. WR77sc (A) roughly phases with a 7.63 day period.

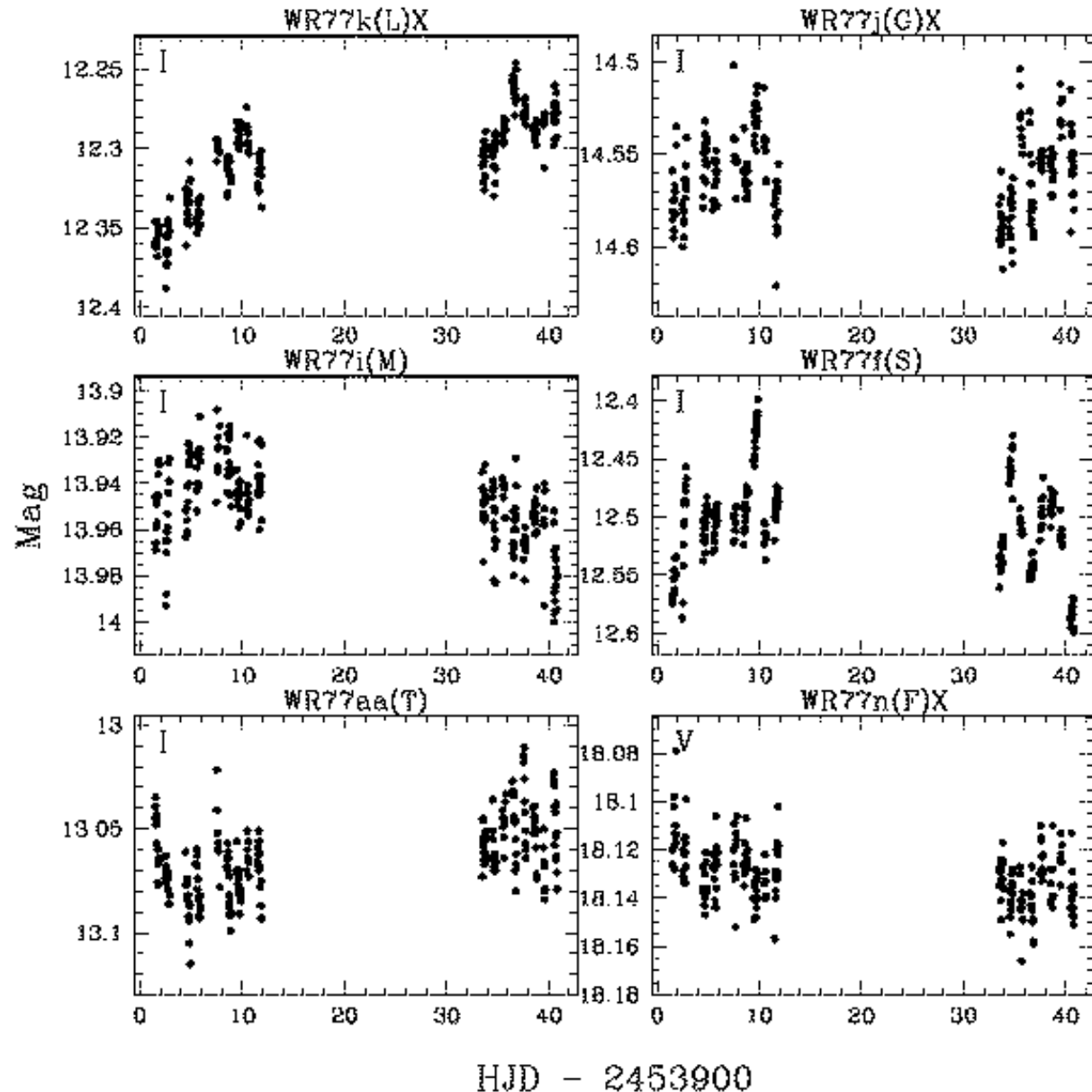


Fig. 4.— Light curves of the other 6 variable Wolf-Rayet members of Westerlund 1. Labels are the same as in Figure 3.

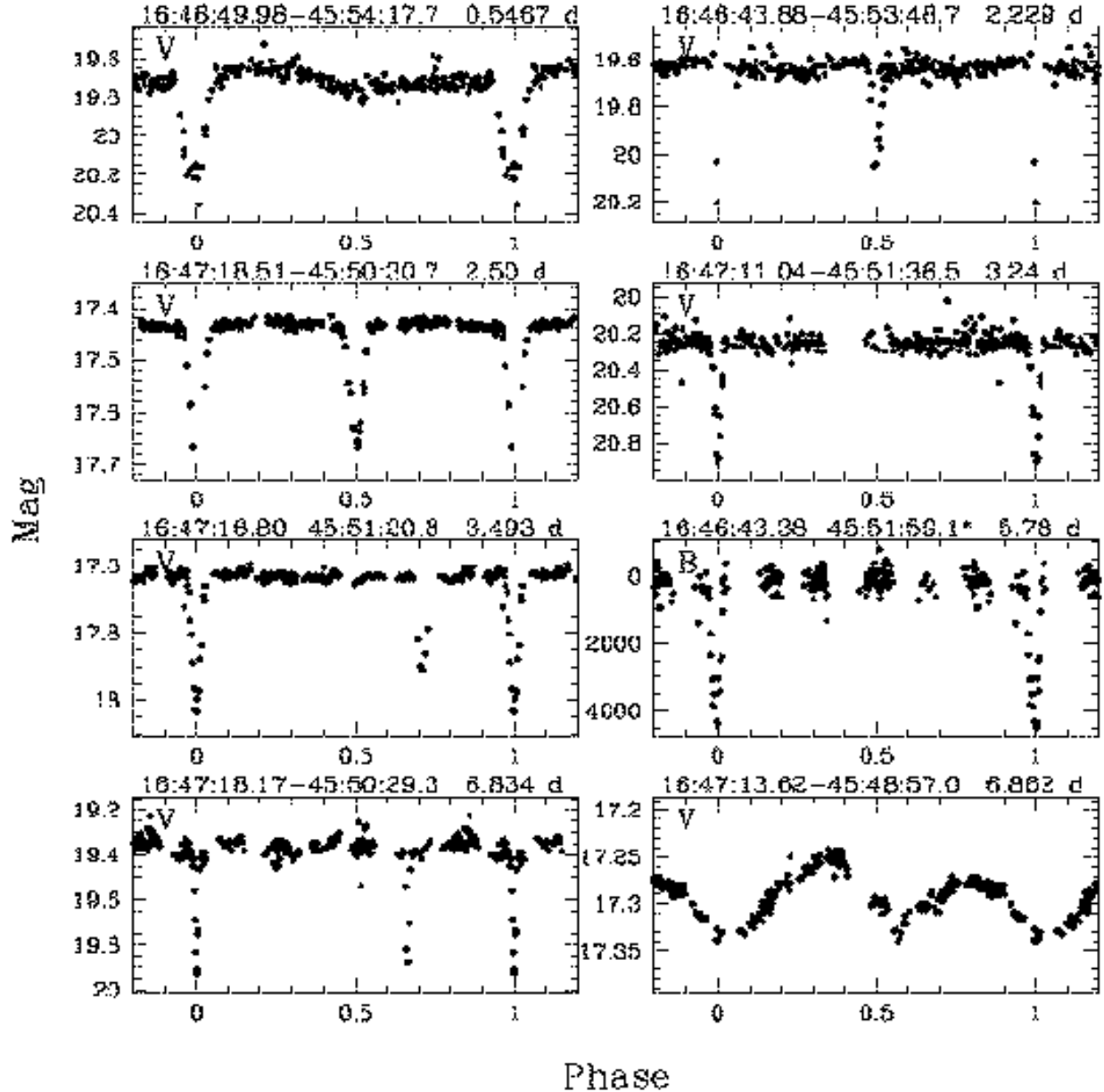


Fig. 5.— Phased light curves of the 7 detached EBs and the RS CVn binary, in order of increasing periods. Their unreddened colors rule out cluster membership. The (RA, Dec) coordinates, periods and filters are labelled. Note that one binary light curve (marked with a *) is given in flux units from the B –band, where it was detected.

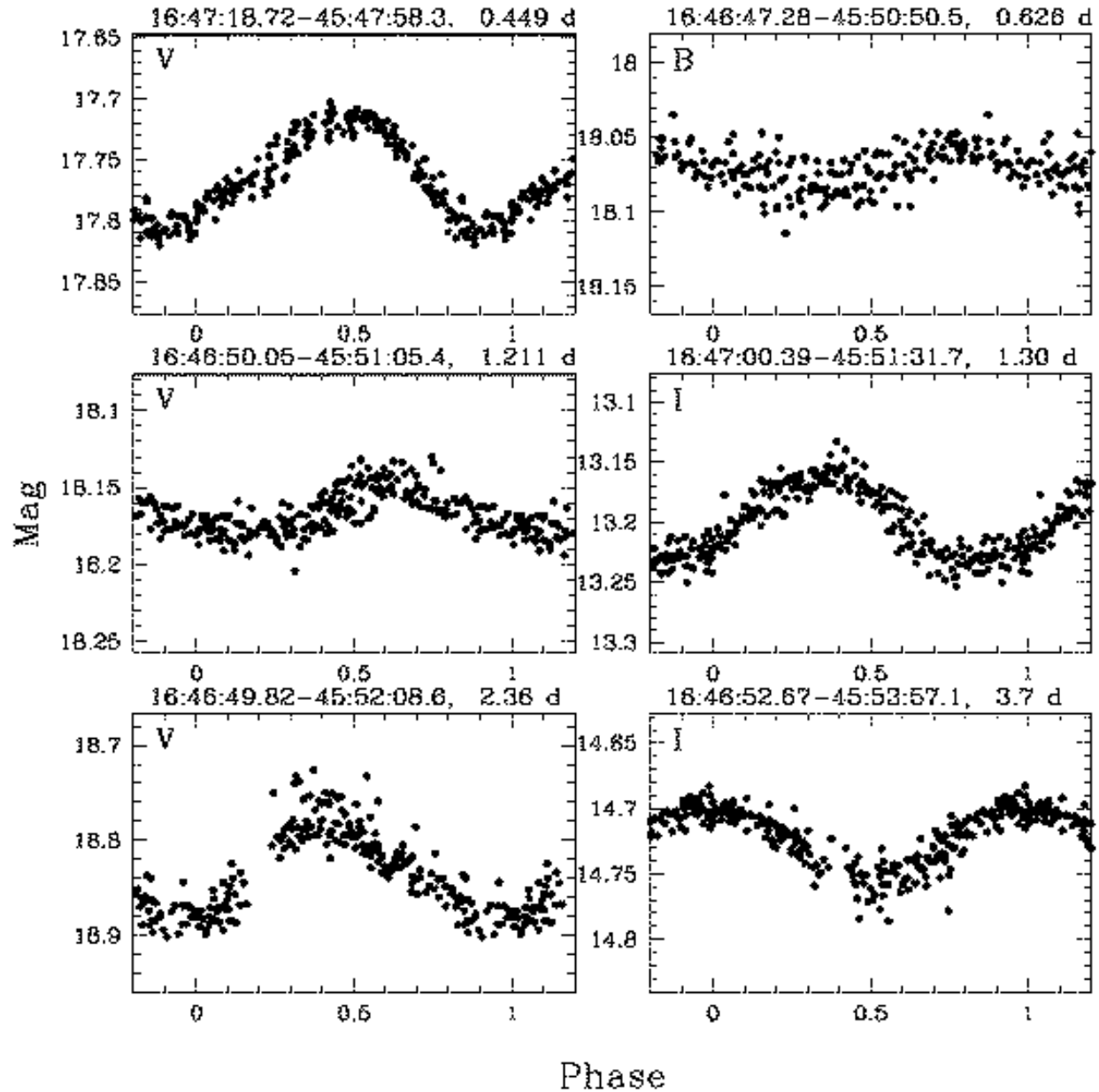


Fig. 6.— Phased light curves of a selection of 6 periodic ($P > 0.2$ day) small-amplitude variables, possibly due to pulsations. The (RA, Dec) coordinates, periods and filters are labelled.

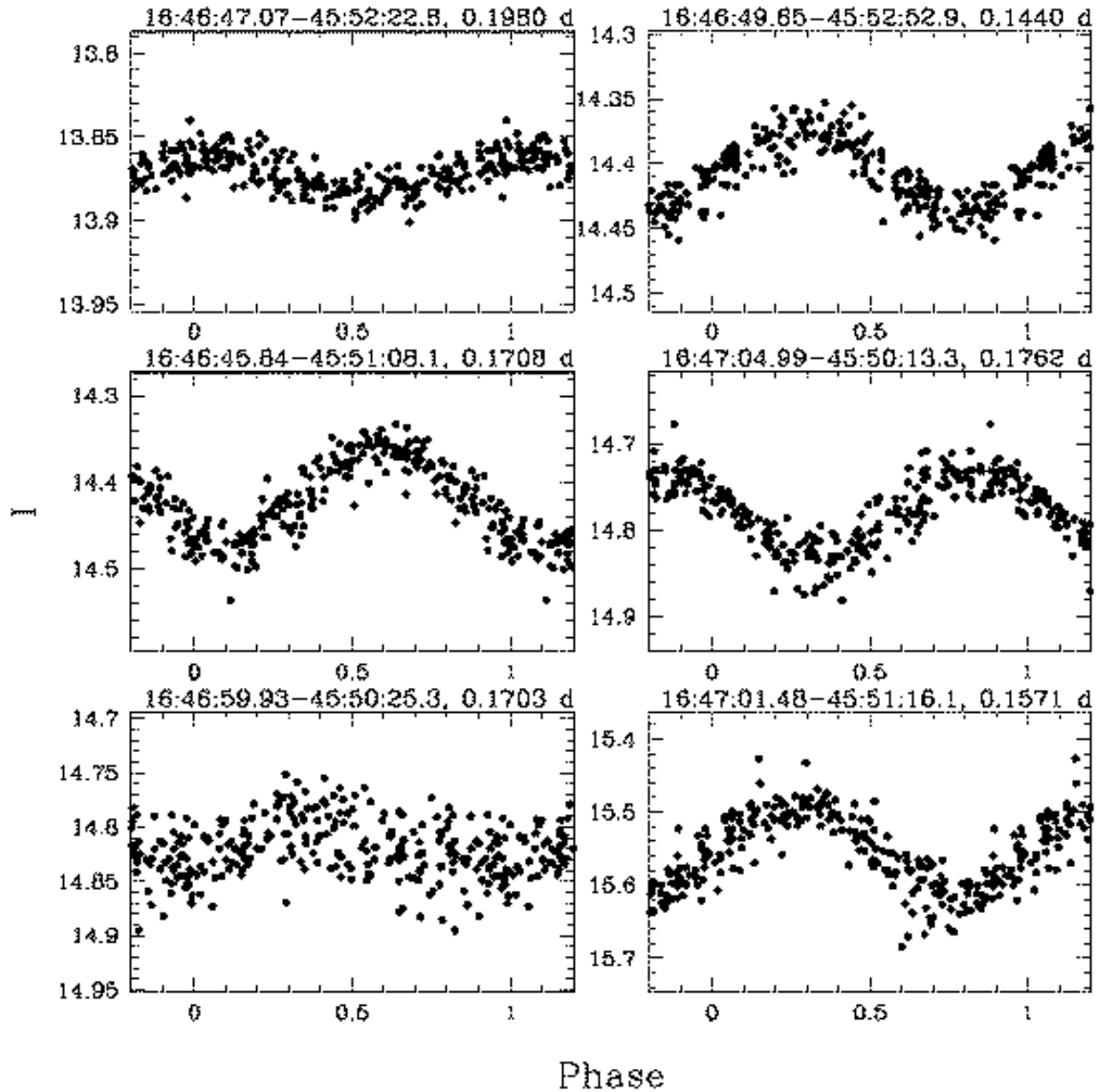


Fig. 7.— Phased I –band light curves of a selection of 6 bright field δ Scuti field variables. The (RA, Dec) coordinates and periods are labelled. The scatter indicates multiple mode pulsations that are typical in such stars.

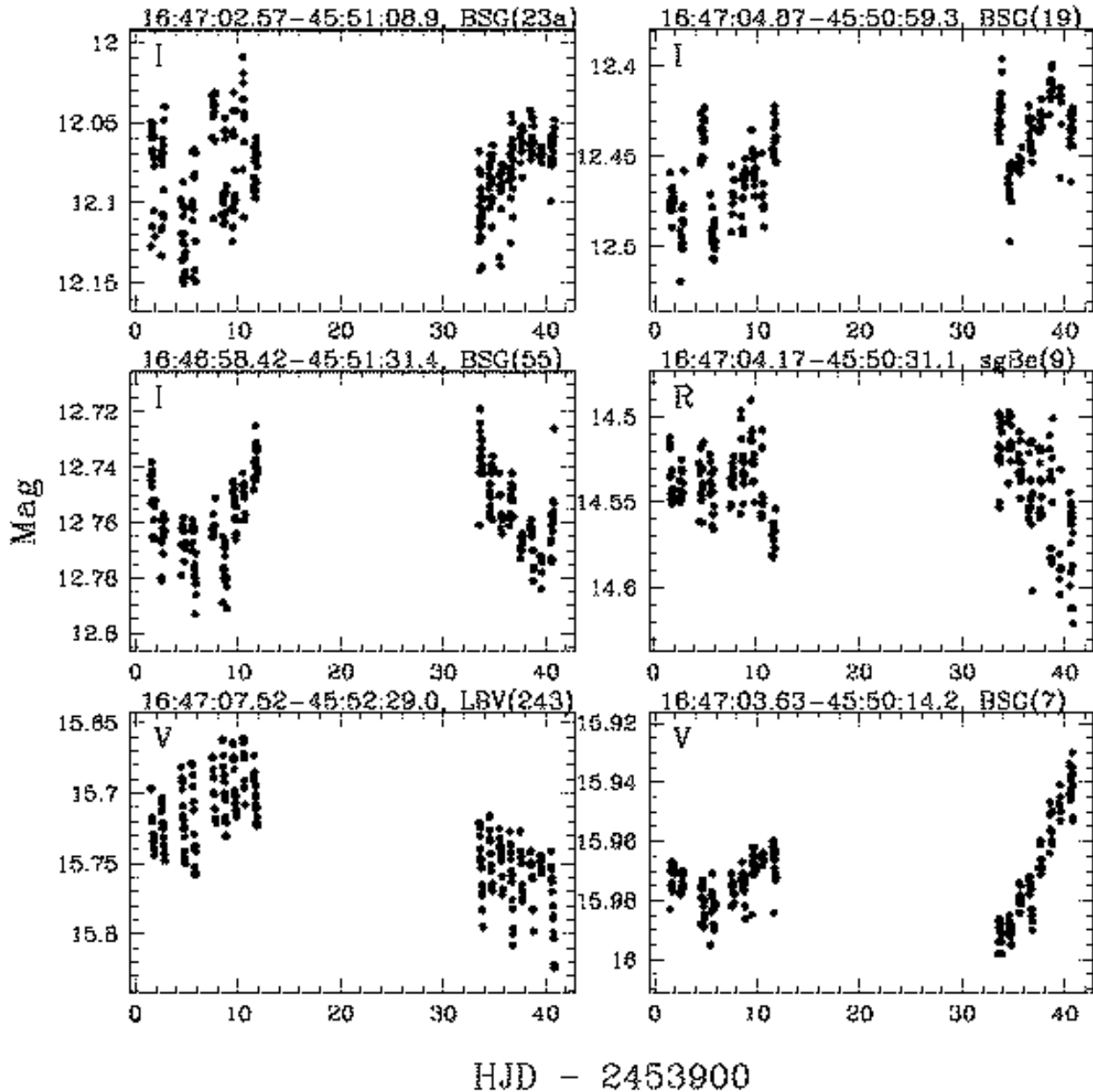


Fig. 8.— Light curves of 6 cluster variables classified as “Other”. The (RA, Dec) coordinates are followed by the spectral classification and Westerlund (1987) name. The filter is labelled in the upper left hand corner.

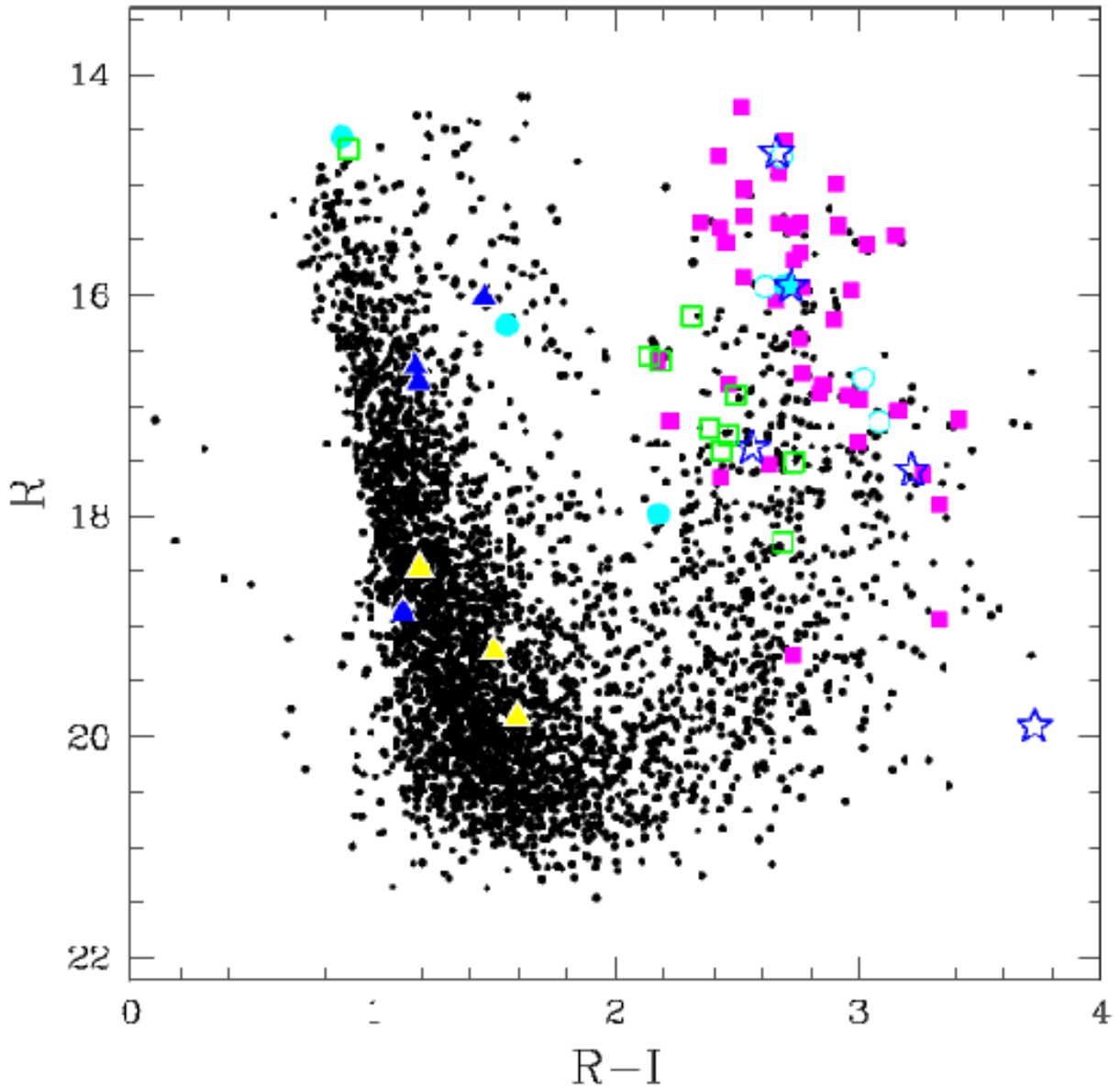


Fig. 9.— R vs. $R - I$ CMD for Westerlund 1 showing the location of the variable stars with light curves in these bands. Cluster and field eclipsing binaries are marked with blue stars and blue filled triangles respectively, δ Scuti with open green squares, W UMa with yellow filled triangles, other long period and semi-regular variables with cyan filled and open circles, respectively. The long period or non-periodic “Other” variables are marked with magenta squares. Many variables, in particular for field stars, were not measured in these bands and are therefore missing from the plot.

REFERENCES

Alard, C. 2000, *A&AS*, 144, 363

Alard, C. & Lupton, R. H. 1998, *ApJ*, 503, 325

Bonanos, A. Z. & Stanek, K. Z. 2003, *ApJ*, 591, L111

Bonanos, A. Z., Stanek, K. Z., Kudritzki, R. P., et al. 2006, *ApJ*, 652, 313

Bonanos, A. Z., Stanek, K. Z., Udalski, A., et al. 2004, *ApJ*, 611, L33

Bopp, B. W. & Stencel, R. E. 1981, *ApJ*, 247, L131

Bromm, V. & Loeb, A. 2006, *ApJ*, 642, 382

Clark, J. S. & Negueruela, I. 2002, *A&A*, 396, L25

Clark, J. S., Negueruela, I., Crowther, P. A., et al. 2005, *A&A*, 434, 949

Crowther, P. A., Hadfield, L. J., Clark, J. S., et al. 2006, *MNRAS*, 1067

Dorfi, E. A., Gautschy, A., & Saio, H. 2006, *A&A*, 453, L35

Fryer, C. L., Mazzali, P. A., Prochaska, J., et al. 2007, preprint (astro-ph/0702338)

Hamuy, M., Folatelli, G., Morrell, N. I., et al. 2006, *PASP*, 118, 2

Hartman, J. D., Bakos, G., Stanek, K. Z., & Noyes, R. W. 2004, *AJ*, 128, 1761

Kobulnicky, H. A., Fryer, C. L., & Kiminki, D. C. 2006, *ApJ*, submitted (astro-ph/0605069)

Krumholz, M. R. & Thompson, T. A. 2006, *ApJ*, submitted (astro-ph/0611822)

Landolt, A. U. 1992, *AJ*, 104, 340

Lefèvre, L., Marchenko, S. V., Moffat, A. F. J., et al. 2005, *ApJ*, 634, L109

Massey, P., Penny, L. R., & Vukovich, J. 2002, *ApJ*, 565, 982

Mengel, S. & Tacconi-Garman, L. E. 2007, *A&A*, in press (astro-ph/0701415)

Monet, D. G., Levine, S. E., Canzian, B., et al. 2003, *AJ*, 125, 984

Muno, M. P., Law, C., Clark, J. S., et al. 2006, *ApJ*, 650, 203

Peeples, M. S., Bonanos, A. Z., DePoy, D. L., et al. 2007, *ApJ*, 654, L61

Pinsonneault, M. H. & Stanek, K. Z. 2006, *ApJ*, 639, L67

Rauw, G., De Becker, M., Naze, Y., et al. 2004, *A&A*, 420, L9

Rauw, G., Vreux, J.-M., Gosset, E., et al. 1996, *A&A*, 306, 771

Schwarzenberg-Czerny, A. 1996, *ApJ*, 460, L107+

Schweickhardt, J., Schmutz, W., Stahl, O., et al. 1999, *A&A*, 347, 127

Skinner, S. L., Simmons, A. E., Zhekov, S. A., et al. 2006, *ApJ*, 639, L35

Stetson, P. B. 1987, *PASP*, 99, 191

—. 2000, *PASP*, 112, 925

van der Hucht, K. A. 2006, *A&A*, 458, 453

Westerlund, B. 1961, *AJ*, 66, 57

Westerlund, B. E. 1987, *A&AS*, 70, 311

Table 1. Transformation coefficients for the Swope CCD.

Instr. Mag.	χ	κ	ξ
$b_{N04}(B-V).....$	2.981 ± 0.009	0.205 ± 0.008	-0.058 ± 0.005
$v_{N04}(B-V).....$	2.892 ± 0.009	0.128 ± 0.007	0.056 ± 0.005
$v_{N04}(V-I).....$	2.888 ± 0.010	0.130 ± 0.008	0.053 ± 0.005
$r_{N04}(V-R).....$	2.766 ± 0.021	0.075 ± 0.017	-0.051 ± 0.014
$i_{N04}(V-I).....$	3.246 ± 0.009	0.055 ± 0.007	-0.042 ± 0.004
$b_{N12}(B-V).....$	3.017 ± 0.016	0.218 ± 0.010	-0.041 ± 0.006
$v_{N12}(B-V).....$	2.890 ± 0.016	0.161 ± 0.010	0.087 ± 0.007
$v_{N12}(V-I).....$	2.886 ± 0.016	0.164 ± 0.010	0.071 ± 0.006
$r_{N12}(V-R).....$	2.789 ± 0.016	0.069 ± 0.010	0.007 ± 0.010
$i_{N12}(V-I).....$	3.189 ± 0.014	0.092 ± 0.008	-0.040 ± 0.005

Table 2. WESTERLUND 1 VARIABLE STAR CATALOG

Name	RA (2000.0)	Dec (2000.0)	$\langle B \rangle$ (mag)	$\langle V \rangle$ (mag)	$\langle R \rangle$ (mag)	$\langle I \rangle$ (mag)	Spectr. Class..	Class.	Period (days)
...	16:47:26.07	-45:50:34.3	...	18.794	Other	...
...	16:47:25.67	-45:54:12.9	18.881	17.333	Other	...
...	16:47:20.83	-45:46:34.1	...	15.719	Other	...
...	16:47:20.75	-45:50:02.6	...	16.961	Other	...
...	16:47:20.37	-45:48:54.7	...	16.523	Other	...
...	16:47:19.50	-45:49:57.3	...	17.605	Other	...
...	16:47:18.72	-45:47:58.3	19.316	17.758	Per	0.449
...	16:47:18.51	-45:50:30.7	19.227	17.450	16.646	15.474	...	DEB	2.50
...	16:47:18.17	-45:50:29.3	...	19.387	DEB	6.834
...	16:47:16.80	-45:51:20.8	19.456	17.650	16.781	15.596	...	DEB	3.493
...	16:47:14.19	-45:48:00.7	...	18.134	Other	...
...	16:47:13.62	-45:48:57.0	19.557	17.289	16.020	14.563	...	EB	6.862
...	16:47:13.39	-45:49:10.5	15.960	12.990	...	Other	...
...	16:47:12.92	-45:47:54.4	21.296	19.397	18.471	17.280	...	WUMa?	0.3657
...	16:47:11.60	-45:49:22.4	16.211	13.314	...	Other	...
...	16:47:11.06	-45:49:30.9	17.729	15.018	...	δ Scuti?	0.144
...	16:47:11.04	-45:51:36.5	...	20.268	DEB	3.24
...	16:47:09.75	-45:51:24.5	19.702	16.694	...	δ Scuti?	0.134
70	16:47:09.39	-45:50:49.6	11.352	B3Ia	Other	...
71	16:47:08.45	-45:50:49.3	...	17.531	14.158	...	B3Ia	Other	...
72,WR77sc(A)	16:47:08.35	-45:50:45.3	16.750	13.728	WN7b,X	Per	7.63
...	16:47:08.24	-45:50:56.4	17.123	13.710	...	Other	...
...	16:47:07.84	-45:51:47.9	16.940	13.939	...	Other	...
WR77sb(O)	16:47:07.68	-45:52:35.6	16.886	14.047	WN6o,X	Other	...
243	16:47:07.52	-45:52:29.0	19.873	15.730	LBV	Other	...
...	16:47:07.29	-45:50:24.2	16.811	14.346	...	Other	...
74	16:47:07.08	-45:50:12.9	15.835	13.312	...	Other	...

Table 2—Continued

Name	RA (2000.0)	Dec (2000.0)	$\langle B \rangle$ (mag)	$\langle V \rangle$ (mag)	$\langle R \rangle$ (mag)	$\langle I \rangle$ (mag)	Spectr. Class..	Class.	Period (days)
...	16:47:07.01	−45:49:40.1	16.702	13.938	...	Other	...
...	16:47:06.68	−45:47:38.5	...	18.250	14.919	Other	...
16a	16:47:06.63	−45:50:42.1	...	16.248	A2Ia+	Other	...
15	16:47:06.61	−45:50:29.5	...	19.301	OBbinary/blend?	Other	...
13	16:47:06.46	−45:50:26.0	...	17.554	14.707	12.044	OBbinary/blend?	EB	9.20
...	16:47:06.34	−45:48:26.2	...	20.486	19.230	17.733	...	WUMa?	0.371
265	16:47:06.29	−45:49:23.7	...	17.739	F5Ia+	Other	...
WR77r(D)	16:47:06.28	−45:51:26.4	18.935	15.600	WN7o,X	Other	...
...	16:47:06.27	−45:51:03.9	17.150	14.065	...	Per	5.2
14c,WR77q(R)	16:47:06.10	−45:50:22.4	17.652	15.223	WN5o,X	Other	...
241,WR77p(E)	16:47:06.07	−45:52:08.3	...	18.379	15.675	12.940	WC9,X	Other	...
25	16:47:05.82	−45:50:33.2	...	18.205	15.331	12.575	...	Other	...
...	16:47:05.79	−45:51:33.3	19.907	16.182	...	EB	2.26
18	16:47:05.73	−45:50:50.4	...	17.610	14.898	12.228	...	Other	...
69	16:47:05.39	−45:51:30.5	...	16.322	Other	...
WR77o(B)	16:47:05.37	−45:51:04.7	17.588	14.367	WN7o,X	EB	3.51
239,WR77n(F)	16:47:05.21	−45:52:24.8	...	18.130	WC9d,X	Other	...
...	16:47:05.12	−45:51:10.1	17.621	14.354	...	Other	...
36	16:47:05.08	−45:50:55.1	22.989	18.975	15.920	13.199	...	EB	3.18
...	16:47:04.99	−45:50:13.3	17.515	14.782	...	δ Scuti?	0.1762
19	16:47:04.87	−45:50:59.3	...	18.784	15.366	12.452	O9.5Ia-B0.5Ia	Other	...
...	16:47:04.77	−45:49:47.1	18.568	16.896	δ Scuti?	0.115
8a	16:47:04.77	−45:50:24.8	...	15.913	F5Ia+	Other	...
...	16:47:04.69	−45:52:06.8	16.899	14.405	...	δ Scuti?	0.1798
28	16:47:04.63	−45:50:38.4	...	17.146	14.303	...	O9.5Ia-B0.5Ia	Other	...
20	16:47:04.68	−45:51:23.9	15.660	...	<M6I	Other	...
...	16:47:04.55	−45:50:08.5	Other	...

Table 2—Continued

Name	RA (2000.0)	Dec (2000.0)	$\langle B \rangle$ (mag)	$\langle V \rangle$ (mag)	$\langle R \rangle$ (mag)	$\langle I \rangle$ (mag)	Spectr. Class..	Class.	Period (days)
...	16:47:04.52	-45:51:19.4	...	16.556	Other	...
238	16:47:04.41	-45:52:27.6	...	17.820	O9.5Ia-B0.5Ia	Other	...
44,WR77k(L)	16:47:04.21	-45:51:07.1	15.457	12.307	WN9h:,X	Other	...
9	16:47:04.17	-45:50:31.1	...	18.056	14.541	...	sgB[e]	Other	...
33	16:47:04.13	-45:50:48.4	20.090	...	12.803	...	B5Ia+	Other	...
60	16:47:04.13	-45:51:52.1	16.041	13.384	O9.5Ia-B0.5Ia	Other	...
WR77j(G)	16:47:04.03	-45:51:25.1	17.893	14.561	(WN7o)X	Other	...
66,WR77i(M)	16:47:03.96	-45:51:37.6	16.906	13.949	WC9d	Other	...
...	16:47:03.96	-45:52:12.0	17.262	14.797	...	δ Scuti?	0.1337
46	16:47:03.93	-45:51:19.6	15.537	12.499	...	Other	...
...	16:47:03.75	-45:51:12.7	17.042	13.879	...	Other	...
7	16:47:03.63	-45:50:14.2	...	15.972	B5Ia+	Other	...
43a	16:47:03.56	-45:50:57.6	15.378	12.647	O9.5Ia-B0.5Ia	Other	...
10	16:47:03.35	-45:50:34.6	22.720	18.516	15.257	...	O9.5Ia-B0.5Ia	Other	...
42a	16:47:03.25	-45:50:52.1	10.764	B5Ia+?	Other	...
...	16:47:03.24	-45:53:11.1	18.545	15.847	...	δ Scuti?	0.1581
...	16:47:03.11	-45:51:31.1	...	19.167	15.929	13.165	...	Other	...
237	16:47:03.10	-45:52:18.8	...	19.008	13.634	...	jM6I	Other	...
6	16:47:03.06	-45:50:23.8	...	18.814	15.928	13.313	O9.5Ia-B0.5Ia	Per	2.20
5,WR77f(S)	16:47:02.96	-45:50:19.7	21.552	17.792	15.035	12.508	WN10-11h/B0-1Ia+	Other	...
...	16:47:02.71	-45:50:23.9	19.651	Other	...
...	16:47:02.69	-45:50:50.3	15.340	12.669	...	Other	...
23a	16:47:02.57	-45:51:08.9	...	18.316	14.986	12.081	O9.5Ia-B0.5Ia	Other	...
48	16:47:02.46	-45:51:24.9	16.818	13.966	...	Other	...
...	16:47:02.32	-45:51:15.2	17.536	14.902	...	Other	...
61a	16:47:02.30	-45:51:41.8	...	17.506	14.633	...	O9.5Ia-B0.5Ia	Other	...
11	16:47:02.25	-45:50:47.1	...	17.508	14.599	11.898	O9.5Ia-B0.5Ia	Other	...

Table 2—Continued

Name	RA (2000.0)	Dec (2000.0)	$\langle B \rangle$ (mag)	$\langle V \rangle$ (mag)	$\langle R \rangle$ (mag)	$\langle I \rangle$ (mag)	Spectr. Class..	Class.	Period (days)
12a	16:47:02.23	−45:50:59.0	...	17.575	13.611	...	A5Ia+	Other	...
49	16:47:01.91	−45:50:31.6	16.392	13.638	...	Other	...
52	16:47:01.85	−45:51:29.4	...	17.876	14.745	12.065	...	Per	6.7
...	16:47:01.69	−45:52:57.8	15.393	12.966	...	Other	...
78	16:47:01.56	−45:49:57.9	...	17.413	14.621	Other	
...	16:47:01.48	−45:51:16.1	18.240	15.553	...	δ Scuti?	0.1571
4	16:47:01.42	−45:50:37.4	18.781	F2Ia+	Other	...
...	16:47:01.44	−45:52:35.0	15.334	12.989	...	Other	...
57a	16:47:01.36	−45:51:45.6	...	16.877	B3Ia	Other	
21	16:47:01.13	−45:51:13.4	15.619	12.861	...	Other	...
...	16:47:00.88	−45:51:20.4	17.336	14.340	...	Other	...
...	16:47:00.52	−45:48:29.7	17.981	15.806	...	Per	1.089
...	16:47:00.54	−45:52:23.3	17.905	Other	...
53	16:47:00.39	−45:51:31.7	...	18.950	15.901	13.198	...	Per	1.30
...	16:46:59.93	−45:50:25.3	17.206	14.818	...	δ Scuti?	0.1703
...	16:46:59.77	−45:51:40.0	19.264	16.536	...	Other	...
2a	16:46:59.71	−45:50:51.2	...	16.978	14.287	11.771	O9.5Ia-B0.5Ia	Other	...
...	16:46:58.97	−45:50:17.8	19.188	17.650	Other	...
...	16:46:58.78	−45:54:31.9	...	20.313	17.377	14.816	...	DEB	4.43
55	16:46:58.42	−45:51:31.4	...	18.030	15.283	12.758	O9.5Ia-B0.5Ia	Other	...
...	16:46:57.71	−45:53:20.0	14.741	12.318	...	Other	
...	16:46:56.89	−45:52:04.4	17.141	14.917	...	Other	...
...	16:46:54.45	−45:53:30.0	17.408	14.975	...	δ Scuti?	0.1271
...	16:46:53.44	−45:53:00.3	...	18.061	16.598	14.425	...	Other	
...	16:46:52.67	−45:53:57.1	...	16.804	16.274	14.724	...	Per	3.7
...	16:46:52.24	−45:51:15.5	17.941	16.546	Other	
...	16:46:51.70	−45:49:07.9	...	16.289	δ Scuti?	0.4852

Table 2—Continued

Name	RA (2000.0)	Dec (2000.0)	$\langle B \rangle$ (mag)	$\langle V \rangle$ (mag)	$\langle R \rangle$ (mag)	$\langle I \rangle$ (mag)	Spectr. Class..	Class.	Period (days)
...	16:46:50.83	-45:53:02.7	14.568	13.700	...	Per	3.715
...	16:46:50.05	-45:51:05.4	...	18.165	Per	1.211
...	16:46:49.98	-45:54:17.7	21.469	19.730	18.874	17.752	...	EB	0.5467
...	16:46:49.82	-45:52:08.6	...	18.825	Per	2.36
...	16:46:49.65	-45:52:52.9	...	18.887	16.589	14.406	...	δ Scuti?	0.1440
...	16:46:48.38	-45:53:56.6	18.324	15.682	...	δ Scuti?	0.1381
...	16:46:47.28	-45:50:50.5	18.071	Per	0.626
...	16:46:47.07	-45:52:22.8	16.187	13.872	...	δ Scuti?	0.1980
WR77aa(T)	16:46:46.30	-45:47:58.2	15.516	13.063	WC9d	Other	...
...	16:46:46.08	-45:48:44.3	...	17.372	Other	...
...	16:46:45.84	-45:51:08.1	...	18.808	16.548	14.415	...	δ Scuti?	0.1708
...	16:46:43.88	-45:53:48.7	...	19.646	DEB	2.229
...	16:46:43.38	-45:51:59.1	DEB	5.78
...	16:46:42.88	-45:50:39.9	18.383	Other	...
...	16:46:42.32	-45:51:50.4	...	18.115	Other	...
...	16:46:42.10	-45:47:01.7	...	21.391	19.826	18.233	...	WUMa?	0.398
...	16:46:41.74	-45:47:13.8	...	16.647	14.673	13.773	...	δ Scuti?	0.1642
...	16:46:41.65	-45:46:41.1	17.994	δ Scuti?	0.1841
...	16:46:40.03	-45:47:50.4	δ Scuti?	0.1650
...	16:46:40.08	-45:51:07.8	...	18.285	Per	0.738
...	16:46:39.82	-45:47:46.4	16.940	δ Scuti?	0.1642

Table 3. LIGHT CURVES OF VARIABLES IN WESTERLUND 1

Name	Filter	HJD–2450000	mag/flux	$\sigma_{mag}/\sigma_{flux}$
16:47:26.07–45:50:34.3	V	3901.50711	18.798	0.013
16:47:26.07–45:50:34.3	V	3901.53865	18.776	0.011
16:47:26.07–45:50:34.3	V	3901.59942	18.808	0.018
16:47:26.07–45:50:34.3	V	3901.62506	18.779	0.018
16:47:26.07–45:50:34.3	V	3901.65933	18.778	0.019
16:47:26.07–45:50:34.3	V	3901.70142	18.776	0.019
16:47:26.07–45:50:34.3	V	3901.74311	18.788	0.020
16:47:26.07–45:50:34.3	V	3901.77163	18.770	0.019
16:47:26.07–45:50:34.3	V	3901.79786	18.774	0.023

Note. — Table 3 is available in its entirety in the electronic version of the Astronomical Journal. A portion is shown here for guidance regarding its form and content.